Figure S1 (related to Figure 1)

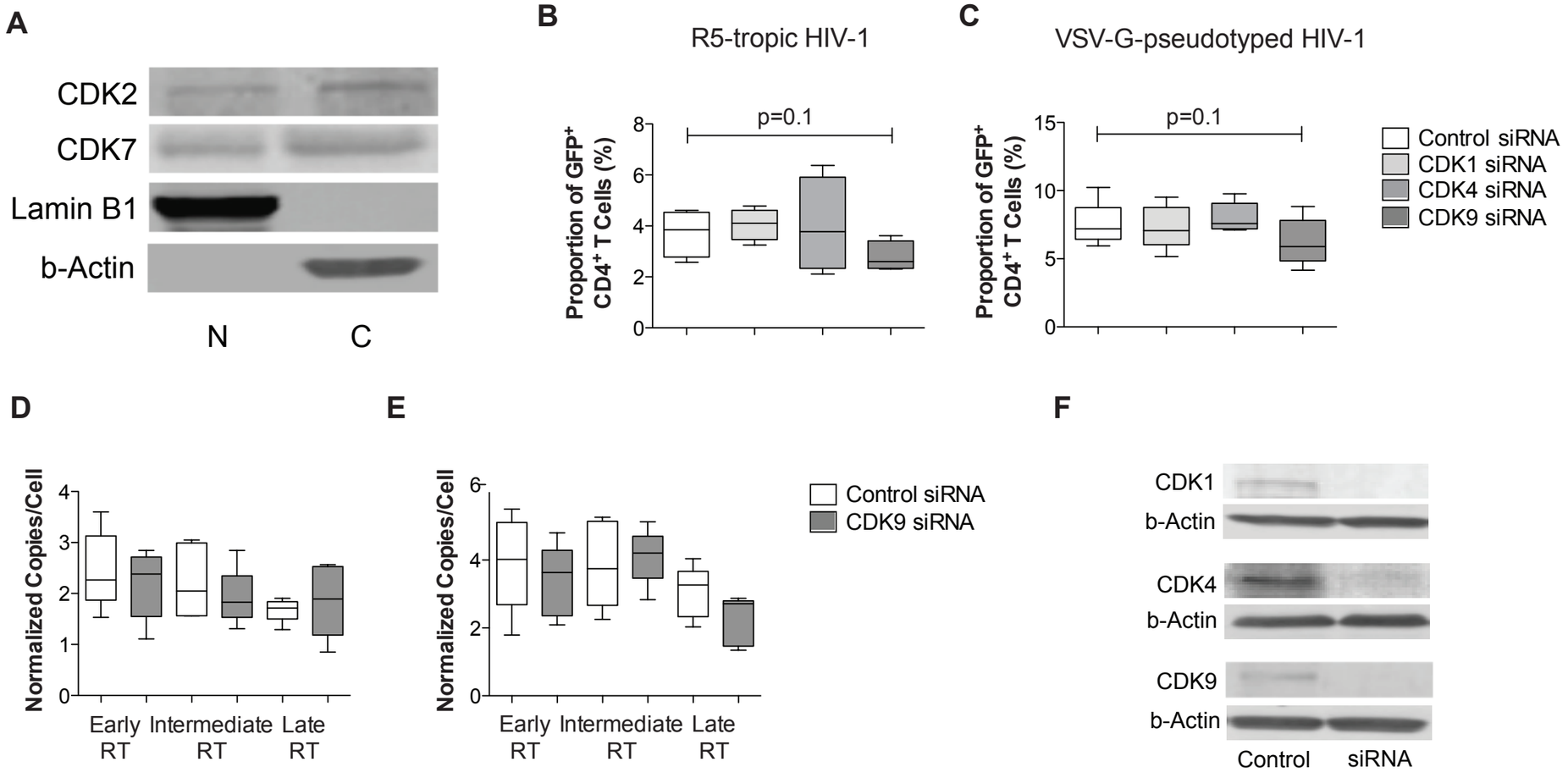

Figure S2 (related to Figure 2)

A

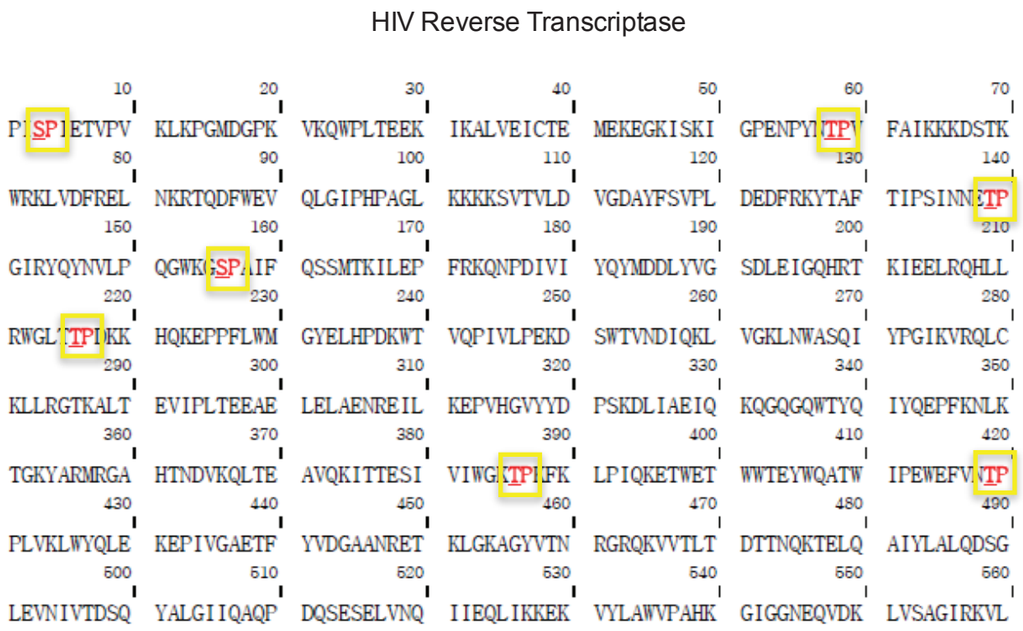

B

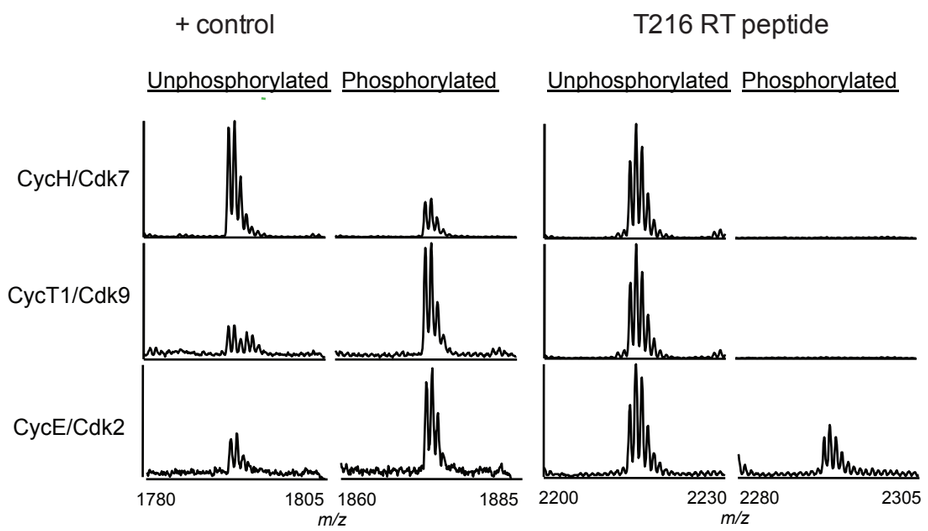

C

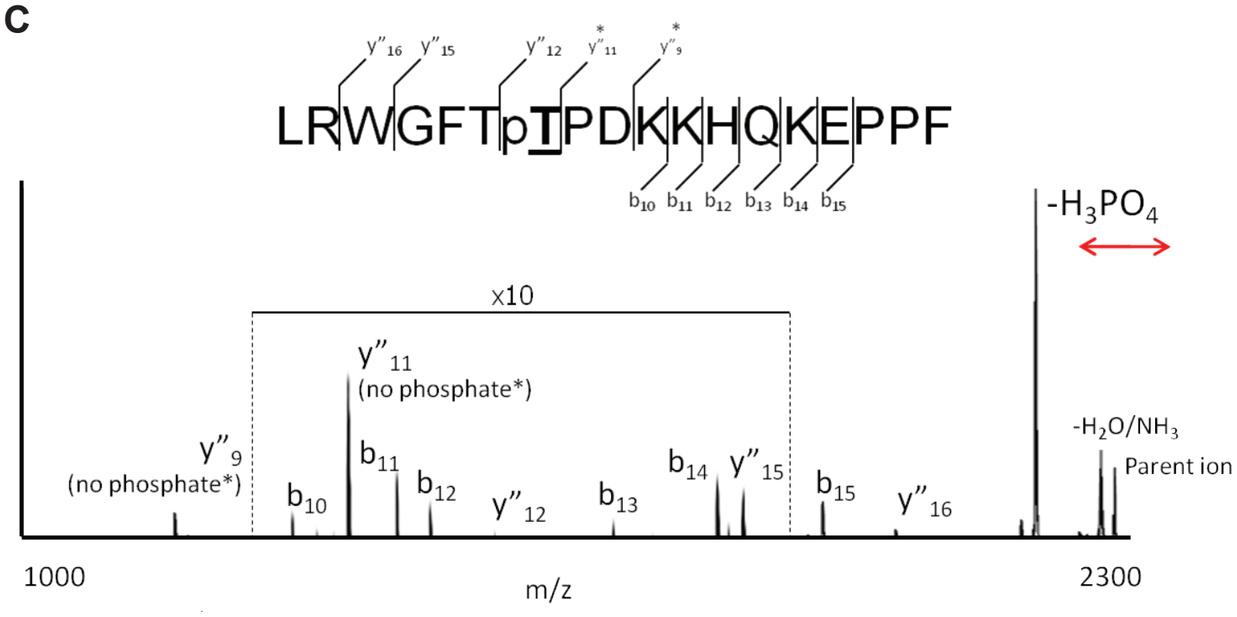

D

Ion	*m/z*	Sequence
y"9	1138.68	KKHQKEPPF
y"11	1350.71	PDKKHQKEPPF
b10	1282.62	LRWGFT**pT**PDK
b11	1410.72	LRWGFTp**T**PDKK
b12	1547.78	LRWGFT**pT**PDKKH
y"12	1531.76	**pT**PDKKHQKEPPF
b13	1675.83	LRWGFT**pT**PDKKHQ
b14	1803.93	LRWGFT**pT**PDKKHQK
y"15	1836.90	GFT**pT**PDKKHQKEPPF
b15	1932.97	LRWGFT**pT**PDKKHQKE
y"16	2022.98	WGFT**pT**PDKKHQKEPPF

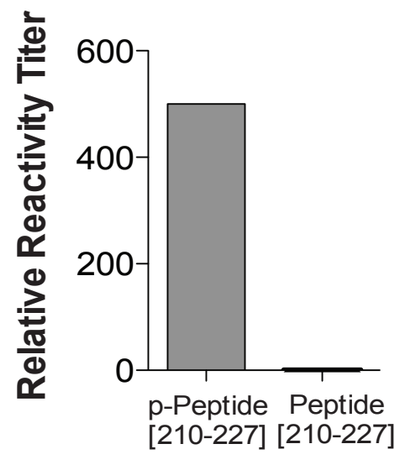

E

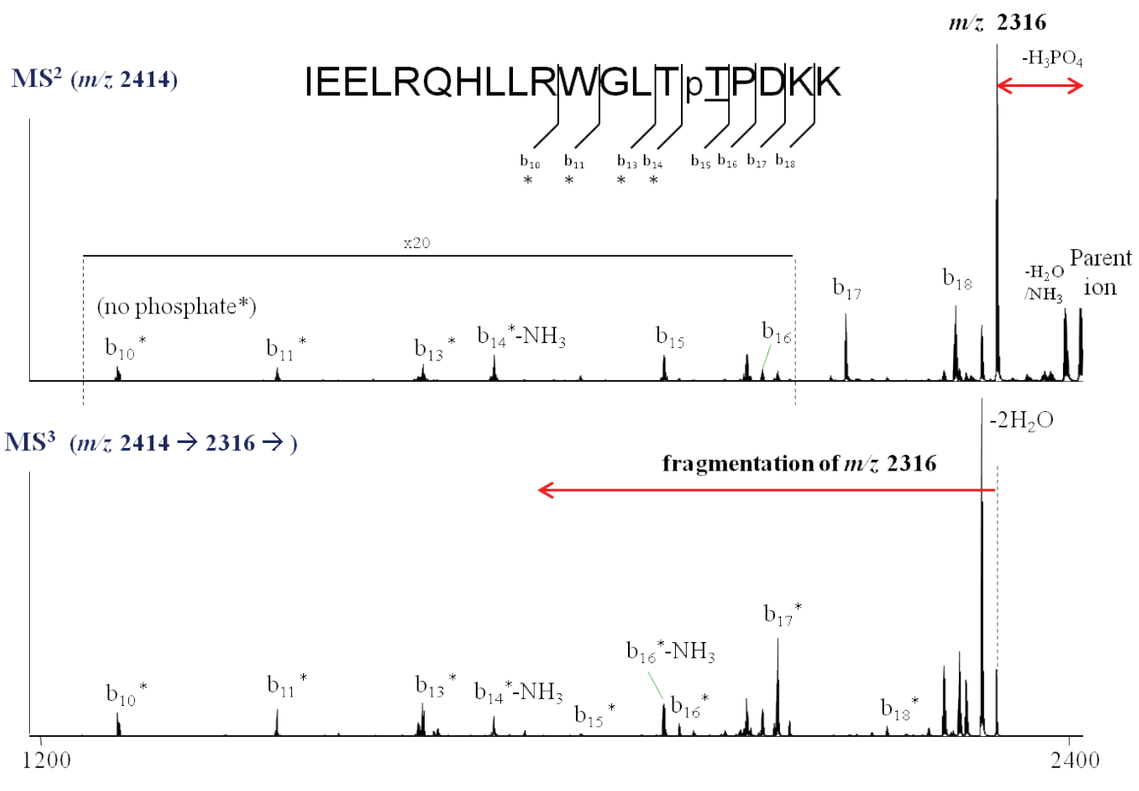

		MS²			MS³
Ion	*m/z*	Sequence	Ion	*m/z*	Sequence
b10*	1288.74	IEELRQHLLR	b10*	1288.74	IEELRQHLLR
b11*	1474.82	IEELRQHLLRW	b11*	1474.82	IEELRQHLLRW
b13*	1644.92	IEELRQHLLRWGL	b13*	1644.92	IEELRQHLLRWGL
b14*	1745.97	IEELRQHLLRWGLT	b14*	1745.97	IEELRQHLLRWGLT
b15	1847.02	IEELRQHLLRWGLT**pT**	b15*	1767.02	IEELRQHLLRWGLTT
b16	1944.07	IEELRQHLLRWGLT**pT**P	b16*	1864.07	IEELRQHLLRWGLTTP
b17	2059.10	IEELRQHLLRWGLT**pT**PD	b17*	1979.10	IEELRQHLLRWGLTTPD
b18	2187.19	IEELRQHLLRWGLT**pT**PDK	b18*	2107.19	IEELRQHLLRWGLTTPDK

Figure S3 (related to Figure 4)

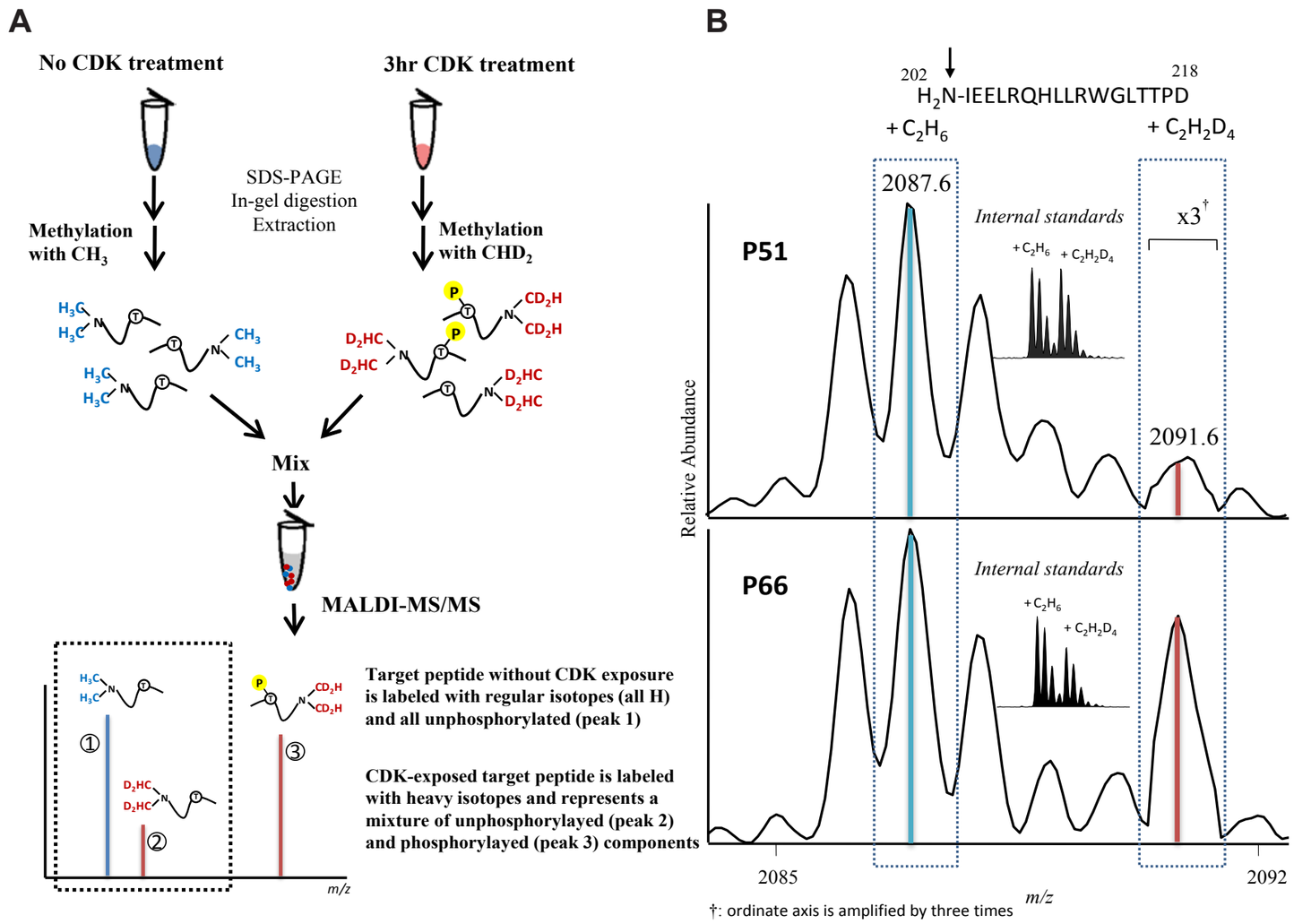

C

Sequence range	MS² fragment sequence	dimethylated (+C_2H_6)	dimethylated (+$C_2H_2D_4$)	p51	p66
Internal standards		*m/z* $[M+H]^+$		D/H	
105-126	AYFSVPLDEDFRK	1615.5	1619.4	0.82	0.58
	VGDAYFSVPLDEDFRK	1886.5	1890.5	0.90	0.58
83-101	FWEVQLGIPHPAGLK	1720.5	1724.5	0.87.	0.51
			Internal Standard Average:	***0.86***	***0.56***
RT samples		*m/z* $[M+H]^+$		D/H	
202-220	IEELRQHLLRWGLTTPD	2086.6	2090.6	***0.07***	***0.21***
			% phosphorylation* :**	**92.3**	**62.1**
			R.S.D. (%):**	**3.2**	**4.9**

* % phosphorylation $= \left[1 - \left(\frac{^{D}/_{H}\ ratio\ for\ RT}{^{D}/_{H}\ ratio\ for\ internal\ standard}\right)\right] \times 100\ \%$

** relative standard deviation, n= 5 measurements

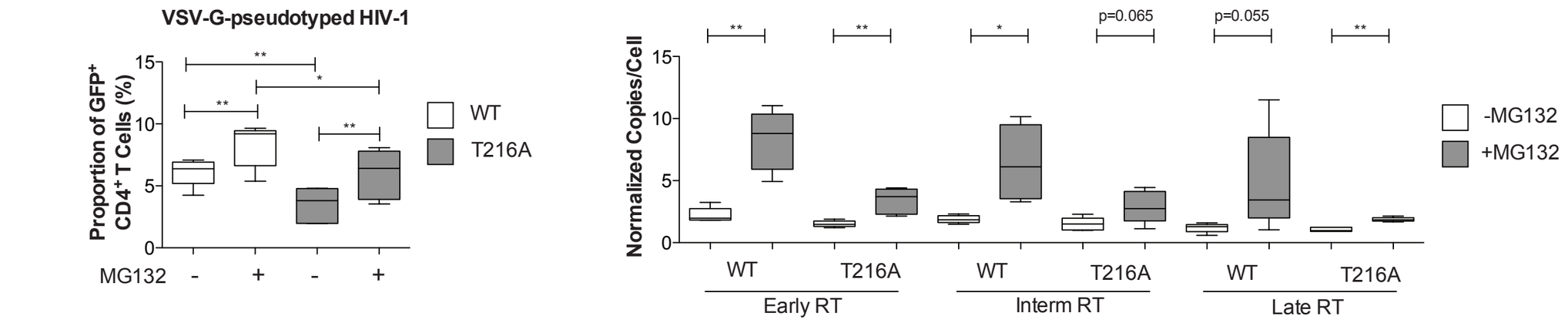

Figure S4 (related to Figure 5)

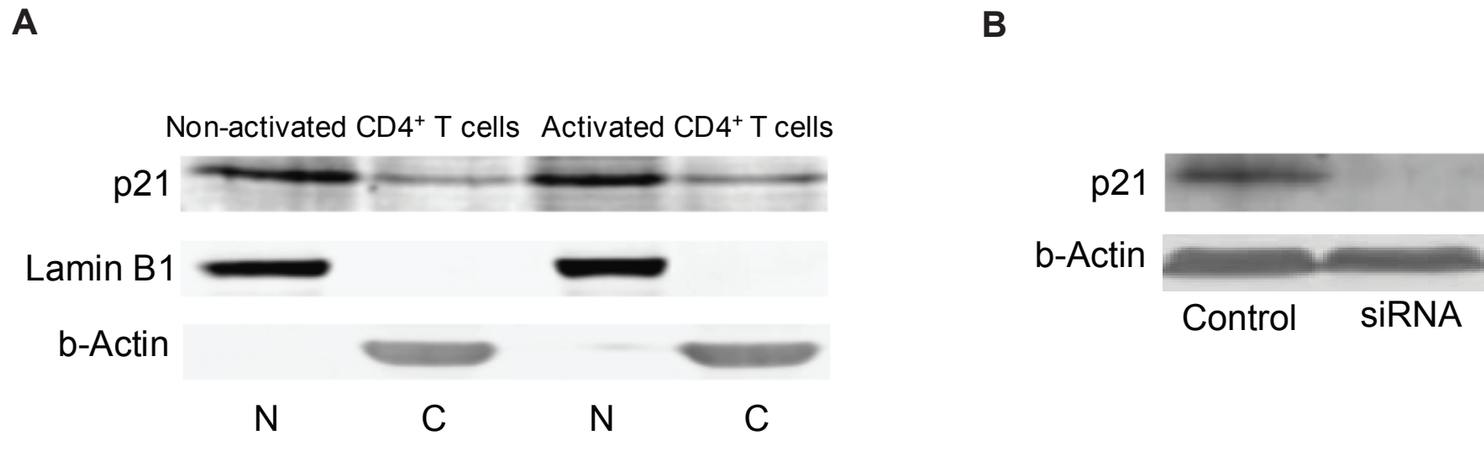

Supplemental figure legends

Supplemental Figure 1 (related to Figure 1): Host CDK2 supports HIV-1 reverse transcription. (A): Subcellular localization of CDK2 and CDK7 in activated $CD4^+$ T cells. Nuclear ("N") and cytoplasmic ("C") protein fractions were isolated from activated $CD4^+$ T cells. Western blots using antibodies directed against CDK2 and CDK7 are shown. Lamin B1 and b-Actin were used as controls for nuclear and cytoplasmic proteins, respectively. (B-C): Infection of $CD4^+$ T cells from HIV-1 negative persons with R5-tropic (B) or VSV-G-pseudotyped (C) HIV-1 in the presence of indicated siRNA. (D-E): Analysis of HIV-1 reverse transcripts in $CD4^+$ T cells infected with R5-tropic (D) or VSV-G pseudotyped (E) HIV-1 after experimental knock-down of CDK9. (F): Detection of CDK1, CDK4 and CDK9 in $CD4^+$ T cells by western blots after siRNA-mediated silencing of the respective genes.

Supplemental Figure 2 (related to Figure 2): HIV-1 RT is a substrate for CDK2-dependent phosphorylation. (A): Seven minimal CDK phosphorylation consensus motifs (S/T)P are highlighted in red in the HIV-1 RT sequence. (B): *In vitro* phosphorylation reaction of synthetic peptide [210-227] by cyclin-dependent kinases. The peptide [210-227] was incubated with ATP and cyclinH/CDK7, cyclinT1/CDK9, or cyclinE/CDK2 for 3 hours, and assayed by MALDI-selected ion monitoring mass spectrometry. Phosphorylation is not observed for CDK7 or CDK9. Dyrktide was used as a positive control. (C): MS^2 spectrum of the phosphorylated synthetic peptide [210-227] analyzed using MALDI-LTQ-MS. MS^2 fragmentation reveals a strong neutral loss of 98 *m/z* units, corresponding to phosphoric acid, characteristic of Ser/Thr phosphorylated peptide ions (McLachlin and Chait, 2001). The signals with *m/z* of the backbone fragmentation indicated that the underlined Threonine residue is phosphorylated. b ions indicate N-terminal peptide fragments and y'' ions indicate C-terminal peptide fragments, both with cleavage at the peptide bond (Biemann, 1990). Phosphate observed in the y''_{11} but not the y''_{12} ion indicates the phosphate group is on the Threonine in the seventh, not the sixth, position in the sequence, which corresponds to Thr216 in the RT sequence. (D): Selective recognition of the phosphorylated HIV-1 RT [210-227] peptide by custom-

made, rabbit-derived antibodies. Rabbits were immunized with the phosphorylated RT [210-227] peptide, and antibodies reactive with the target peptide were purified according to standard procedures, followed by negative absorption with the unphosphorylated RT [210-227] peptide. Purity of isolated phospho-specific antibody was tested by indirect Elisa assays against the phosphorylated or unphosphorylated [210-227] RT peptides bound individually to solid phase columns. Elutions from both columns were selectively tested for reactivity with the phosphorylated RT [210-227] peptide. Relative reactivity titers of the eluents from each column with the phosphorylated RT [210-227] peptide are indicated. (E): MS^2 and MS^3 spectra of Thr216 [202-220] phosphorylated Lys-C proteolytic RT peptide. In MS^2 spectrum, a strong neutral loss of phosphoric acid indicated the presence of phosphate, and the minor peaks representing backbone fragmentation showed the phosphorylation occurs on the underlined Threonine (in the CDK motif). *m/z* consistent with phosphorylation on the b_{15} ion but not he b_{14} ion indicates that the phosphate group is on the Threonine at the 15^{th} position, which corresponds to Thr216 in the RT sequence. MS^3 fragmentation of *m/z* 2316 (loss of phosphate in MS^2) confirmed the sequence of phosphorylated peptide, by presenting backbone fragmentation consistent with the 202-220 peptide, but without phosphate addition.

Supplemental Figure 3 (related to Figure 4): CDK2-dependent phosphorylation increases function and stability of HIV-1 RT. (A-C): HIV Quantification of in vitro phosphorylation of HIV-1 RT. (A): Relative quantification of specific chemical species in two samples can be achieved by using stable isotope labeling in conjunction with mass spectrometry (Oda et al., 1999; Pan and Aebersold, 2007). This requires that one sample be chemically modified with a heavy, stable isotope-containing chemical group, while the second sample be modified with the same chemical group that contains only regular isotopes. The two samples are then mixed. Mass spectrometry can distinguish the heavy isotope species from the first sample, and the corresponding regular isotope species from the second sample. The relative amounts of that species are then simply obtained from the heavy:light peak intensity ratio. In this experiment, isotope is introduced as deuterated methyl groups after in-gel proteolysis. Free amines from lysine side chains and peptide

N-termini are dimethylated either with regular hydrogen-containing methyl groups (2 x CH_3, for the unphosphorylated sample) or with doubly-deuterated methyl groups (2 x CD_2H, for the phosphorylated sample). The regular isotope-labeled unphosphorylated RT peptides are then mixed with the heavy isotope-labeled phosphorylated RT peptides, and subjected to MALDI-MS analysis. Relative quantification of T216 phosphorylation is determined by measuring the decrease in the abundance of unphosphorylated proteolyic peptide fragment ion spanning residues 202-218. (B) Peak intensity of the unphosphorylated T216-containing peptide is decreased for deuterated, Cdk-treated RT (red bar, *m/z* = 2091.6) relative to regular, RT with no kinase treatment (blue bar, *m/z* = 2087.6). These measurements are obtained from the b_{17} fragment ion spanning RT residues 202-218 arising from the MS^2 fragmentation of Lys-C proteolytic peptide spanning residues 202-220. The MS^2 fragment ions are used to increase specificity and decrease chemical noise. Quantitative results are derived as the second isotope after deconvolving the overlapping isotope distributions of the H- and D-containing peptides. Similar results are obtained for other, less intense fragment ions of the same parent peptide (not shown). Internal standard spectra (inset) are used to correct for potential differences in peptide recovery. (C) Dimethyl-based stable isotope is used to determine *in vitro* phosphorylation stoichiometry for the p51 and p66 subunits of HIV-RT. (D-E): HIV-1 infection in the presence of proteasome inhibitors. (D): Infection of $CD4^+$ T cells from HIV-1 negative persons with VSV-G-pseudotyped HIV-1 in the presence or absence of proteasome inhibitors (MG132). (E): Corresponding analysis of HIV-1 reverse transcripts after infection of $CD4^+$ T cells in the presence or absence of MG132.

Supplemental Figure 4 (related to Figure 5): Inhibition of p21 (waf-1/cip-1) increases HIV-1 reverse transcription in $CD4^+$ T cells from elite controllers. (A): Subcellular localization of p21 in non-activated $CD4^+$ and activated $CD4^+$ T cells. Detection of p21 in nuclear ("N") and cytoplasmic ("C") protein fractions from non-activated $CD4^+$ and activated $CD4^+$ T cells by western blots. Lamin B1 and b-Actin were used as controls. (B): Efficacy of p21 siRNA-mediated gene silencing. Detection of p21 protein in $CD4^+$ T cells after siRNA-mediated silencing of the respective gene. b-Actin was used as control.

References

Biemann, K. (1990). Appendix 5. Nomenclature for peptide fragment ions (positive ions). Methods Enzymol *193*, 886-887.

McLachlin, D.T., and Chait, B.T. (2001). Analysis of phosphorylated proteins and peptides by mass spectrometry. Curr Opin Chem Biol *5*, 591-602.

Oda, Y., Huang, K., Cross, F.R., Cowburn, D., and Chait, B.T. (1999). Accurate quantitation of protein expression and site-specific phosphorylation. Proc Natl Acad Sci U S A *96*, 6591-6596.

Pan, S., and Aebersold, R. (2007). Quantitative proteomics by stable isotope labeling and mass spectrometry. Methods Mol Biol *367*, 209-218.